

Article

FT-MIR Analysis of Water-Soluble Extracts during the Ripening of Sheep Milk Cheese with Different Phospholipid Content

Lambros Sakkas ^{1,*}, Christos S. Pappas ² and Golfo Moatsou ¹ 

¹ Laboratory of Dairy Research, Department of Food Science and Human Nutrition, Agricultural University of Athens, 11855 Athens, Greece; mg@hua.gr

² Laboratory of Chemistry, Department of Food Science and Human Nutrition, Agricultural University of Athens, 11855 Athens, Greece; chrispap@hua.gr

* Correspondence: lasakkas@hotmail.com

Abstract: The purpose of this work was to study the suitability of the water-soluble extracts (WSE) of semi-hard sheep milk cheese for analysis by diffuse reflectance Fourier transform mid-infrared spectroscopy (FT-MIR) and the development of classification models using discriminant analysis and based on cheese age or phospholipid content. WSE was extracted from three types of sheep milk cheeses (full-fat, reduced-fat and reduced-fat fortified with lyophilized sweet sheep buttermilk) at various stages of ripening from six to 168 days and lyophilized. The first model used 1854–1381 and 1192–760 cm⁻¹ regions of the first-derivative spectra and successfully differentiated samples of different age, based on changes in the water-soluble products of ripening biochemical events. The second model used the phospholipid absorbance spectral regions (3012–2851, 1854–1611 and 1192–909 cm⁻¹) to successfully discriminate cheeses of markedly different phospholipid content. Cheese WSE was found suitable for FT-MIR analysis. According to the results, a fast and simple method to monitor cheese ripening based on water-soluble substances has been developed. Additionally, the results indicated that a considerable amount of phospholipids migrates to the cheese WSE and that FT-MIR can be a useful tool for their assessment.

Keywords: FT-MIR cheese spectra; cheese ripening; cheese phospholipids; sheep milk cheese; water-soluble extract



Citation: Sakkas, L.; Pappas, C.S.; Moatsou, G. FT-MIR Analysis of Water-Soluble Extracts during the Ripening of Sheep Milk Cheese with Different Phospholipid Content. *Dairy* **2021**, *2*, 530–541.

<https://doi.org/10.3390/dairy2040042>

Academic Editor:
Antonio-José Trujillo

Received: 22 August 2021

Accepted: 16 September 2021

Published: 23 September 2021

Publisher's Note: MDPI stays neutral with regard to jurisdictional claims in published maps and institutional affiliations.



Copyright: © 2021 by the authors. Licensee MDPI, Basel, Switzerland. This article is an open access article distributed under the terms and conditions of the Creative Commons Attribution (CC BY) license (<https://creativecommons.org/licenses/by/4.0/>).

1. Introduction

Infrared spectroscopy is based on the measurement of infrared light absorption by a sample, corresponding to the vibrations of the chemical bonds in its molecules [1,2]. The main spectral regions used in the analysis of dairy products are the near-infrared (NIR, 14,000–4000 cm⁻¹) and the mid-infrared (MIR, 4000–400 cm⁻¹) regions [1,3]. MIR spectroscopy exhibits higher signal and structural sensitivity and higher repeatability compared to NIR analysis [4]. Fourier transform mid-infrared spectroscopy (FT-MIR) is a fast, non-complicated and non-destructive analytical procedure which is advantageous for the in-depth study of protein structure [2,5].

It has been used in many studies to determine composition—i.e., cheddar cheese [6], Swiss cheese [7]—or chemical parameters in several kinds of cheeses—i.e., Emmental cheese [8], soft cheeses, [9]—or short-chain free fatty acid content in Swiss cheese [10], or for the evaluation of flavour quality in cheddar [6,11] and Swiss cheese [12] or in the rapid estimation of microbial counts in Feta cheese [13]. Different manufacturing conditions have been related with distinct FT-MIR spectral reflectance in pecorino cheese [14], cream cheese [15] and cheese produced from high pressure homogenized or untreated goat milk [16]. The successful determination of the geographic origin has been reported for Emmental [17,18], gruyère and L'Etivaz cheeses [19]. Furthermore, FT-MIR could be a reliable tool for the determination of authenticity of cheeses—as reported for grated Parmigiano

Reggiano [20,21] and for Saint-Nectaire cheese [22]—or the detection of adulteration of cheese with fat of non-dairy origin [23,24].

Monitoring of cheese ripening is very important in cheese quality assessment because the biochemical changes that take place determine to a great extent the final characteristics of the cheese, i.e., moisture, water activity, microstructure, and sensory properties [11,25]. The main phenomena of cheese ripening are proteolysis, lipolysis, catabolism of residual glucose and lactic acid, and further changes of the final products of the processes [26,27]. Evaluation of ripening biochemical events is mainly performed through physicochemical, chromatographic and electrophoretic methods, which are time consuming and expensive. Thus, the implementation of FT-MIR would be of great interest for cheese research and the industry [27,28]. Several researcher groups have detected significant differences in FT-MIR spectral regions—mainly corresponding to protein and lipid functional groups absorption—throughout cheese ageing [29–31], but there are only a few reports for the monitoring of cheese ripening. Dufour et al. [32] discriminated semi-hard cheeses at ripening times of 1, 21, 51 and 81 days by the methylene absorption region ($3000\text{--}2780\text{ cm}^{-1}$). Mazerolles et al. [33] discriminated semi-hard cheeses at the same ripening times by the Amide I and II regions ($1700\text{--}1500\text{ cm}^{-1}$), which also correlated well with the respective chemical analyses data. Cattaneo et al., [34] managed to evaluate the shelf-life of crescent cheese and Martín-del-Campo et al., [35] estimated the ripening day of Camembert-type cheese with one day error. The latter group [36] used FT-MIR to successfully discriminate Emmental cheeses in four groups according to days of ripening, i.e., 21 and 34 days, 51 and 58 days, 65 days or 85 days. Chen et al. [37] categorized Swiss cheeses at different ripening periods up to 90 days by coupling FT-MIR microspectroscopy with multivariate analysis. Subramanian et al., [27] developed prediction models of cheddar cheese age and amino acid and organic acid contents. To our knowledge, similar studies for sheep milk cheese are very scarce. In fact, the application of FT-MIR in the assessment of the ripening stage of sheep milk cheese varieties has been reported only by Andrade et al. [38] who differentiated cheese according to age.

Another challenging approach could be the implementation of FT-MIR in the study of phospholipids of cheese. Phospholipids are amphipolar lipids of milk fat globule membrane, which are considered very important due to their functional and bioactive properties [39,40]. Phospholipid intake through consumption of dairy products is thought to have beneficial nutritional effects on both infants and adults, i.e., they supply choline, ethanolamine and polyunsaturated fatty acids, and potentially hinder cholesterol absorption [40]. Reports for cheese phospholipids are very limited. Analysis is usually performed by means of chromatographic methods, while a first step of extraction is needed prior to analysis [39,41,42]. The procedure is demanding in terms of time and cost, requiring various analytical instrumentation and considerable amounts of organic solvents. Taking into consideration all the above, the development of a relevant FT-MIR method would be of great interest.

Mostly, FT-MIR analysis is performed directly on cheese slices. There are a few reports for the FT-MIR analysis of cheese fractions. Koca et al., [10] analyzed both Swiss cheese and its acidified water extract to determine short-chain free fatty acids. Martín-del-Campo et al., [35] analyzed Camembert-type cheese fractions such as defatted cheese suspension and acid soluble nitrogen extract. Analysis of cheese water/chloroform/ethanol cheese extract has been reported by Subramanian et al., [6,11,27] for cheddar, and by Chen et al., [37] and Kocaoglu-Vurma et al., [12] for Swiss cheese.

Considering the importance of cheese ripening for the final product quality and the demand for a quick, simple and reliable analytical method for ripening assessment, this study was undertaken. The objective was the analysis of the water-soluble extracts (WSE) of semi-hard sheep milk cheese with different fat content, at different ripening or storage stages by means of diffuse reflectance Fourier transform mid-infrared spectroscopy (DRIFTS). FT-MIR analysis was performed on WSE since the products of the biochemical events occurring during cheese ripening are mainly water-soluble. Moreover, with use of

WSN the effect of residual casein and the fat on the spectra is excluded. In addition, the present study aimed to investigate the effect of different phospholipid contents of cheese on the spectra. For this purpose, three types of cheese used in our previous study [42] were analyzed; that is, full-fat, reduced-fat and reduced-fat fortified with sweet sheep buttermilk powder.

2. Materials and Methods

2.1. Cheese Samples and Water-Soluble Extracts

Semi-hard full-fat (FF) and reduced-fat (RF) sheep milk cheeses manufactured at various stages of ripening from six to 168 days were used for water-soluble extraction and analyses. Cheese making and ripening conditions have been reported by Sakkas et al. [42]. The cheese codes were: “A” (FF; 22.37 ± 0.890 g fat/100 g cheese), “B” (RF; 12.52 ± 0.620 g fat/100 g cheese) and “C” (RF fortified at 1% of cheese milk with lyophilized sweet sheep buttermilk; 11.67 ± 0.481 g fat/100 g cheese). The first step of cheese water-soluble extract (WSE) preparation was the homogenization of 20 g cheese in 180 g distilled water at 9500 rpm for 2 min by means of Ultra Turrax (IKA-Werke GmbH & Co. KG, Staufen im Breisgau, Germany). Next, the cheese slurry was heated at 40 °C for 1 h and rehomogenized at 9500 rpm for two min. After immediate cooling, the slurry was centrifuged at $10,000 \times g$, for 10 min, at 4 °C, and the supernatant was filtered through Whatman No 1 filter paper at a temperature lower than 6 °C. WSE filtrate was lyophilized at ≤ -40 °C for 48–72 h using an ALPHA I-12 freeze-dryer (Martin Christ Gefriertrocknungsanlagen GmbH, Osterode am Harz, Germany), prior to FT-MIR analysis.

2.2. FT-MIR Spectroscopy

FT-MIR spectra of WSE were obtained using a Thermo Nicolet 6700 Fourier transform infrared spectrometer (Thermo Electron Corporation, Madison, WI, USA) with a DRIFTS micro sampling cup and a deuterated triglycine sulphate (DTGS) detector (Spectra-Tech Inc., Stamford, CT, USA). Three spectra were collected (from three sub-samples) and an average spectrum was assessed for each WSE sample with a resolution of 4 cm^{-1} and a total of 100 scans. Recording and further processing of spectra were carried out by means of the OMNIC software (OMNIC 8.2.0.387, Thermo Fisher Scientific Inc., Waltham, MA, USA). The Savitzky–Golay algorithm (5-point moving, second-degree polynomial) was used for spectra smoothing and the baseline of all spectra was corrected accordingly (second-degree polynomial, 20 iterations).

2.3. Discriminant Analysis

Initially the samples were placed according to the class to which they belong (actual class). Then, the software calculated an average spectrum for each class and classified the spectra in a class (calculated class) according to the Mahalanobis distance from each averaged spectrum of each class. The standard samples are used for the calibration and the validation samples for internal validation. The standard and validation samples are samples of all classes and their usage as “standard” or “validation” samples is determined by the software. Finally, the models were validated externally (external validation) by a set of external validation samples of all classes other than those used for the calibration and the internal validation. Ten principal components (PC) were used according to Eigen analysis and the Performance Index (PI) was calculated. A high PI value shows a robust model.

2.3.1. Discrimination Model of Ripening Stage

The first-derivative spectra of $1854\text{--}1381\text{ cm}^{-1}$ and $1192\text{--}760\text{ cm}^{-1}$ spectral regions were used for discriminant analysis of samples with TQ Analyst software (version 8.0.0.245, Thermo Fisher Scientific Inc.). The samples were classified in five actual classes, according to their age and coded as “6d” (6 days), “28d” (28 days), “56d” (56 days), “112d” (112 days) and “168d” (168 days). Forty-three samples (seven samples of class 6d, nine samples of class 28d, 13 samples of class 56d, nine samples of class 112d and five samples of class

168d) were used by the software as calibration standards and 15 samples (one sample of class 6d, five samples of class 28d, two samples of class 56d, six samples of class 112d and one sample of class 168d) were used as validation standards. Finally, the calibrated method was validated by an external validation set of six different samples of all classes.

2.3.2. Discrimination Model of Phospholipid Content

The spectral regions of $3012\text{--}2851\text{ cm}^{-1}$, $1854\text{--}1611\text{ cm}^{-1}$ and $1192\text{--}909\text{ cm}^{-1}$ were used for discriminant analysis of the spectra of B and C cheese WSEs with TQ Analyst software. Cheese A was excluded due to its nearly two-fold higher fat content compared to that of cheeses B and C. This would probably result in a quite higher content of free short- and medium-chain fatty acids in the WSE of cheese A compared to that of B and C cheese WSEs. Similarly to phospholipids, fatty acids absorb at $3012\text{--}2851$ and $1854\text{--}1611\text{ cm}^{-1}$ regions and they could complicate the development of the discrimination model by contributing to phospholipid absorbance. Instead, WSEs of cheeses B and C were used, which are both RF cheeses and they are expected to contain similar levels of short- and medium-size fatty acids [42]. The samples were classified in two actual classes, B and C. Twenty-six samples (12 samples of class B and 14 samples of class C) were used by the software as calibration standards and 10 samples (four samples of class B and six samples of class C) were used as validation standards. Finally, the calibrated method was validated by an external validation set of six different samples of both classes. According to Eigen analysis, 10 PC were used.

3. Results

3.1. Spectroscopic Study

3.1.1. Spectral Regions Related to Cheese Ripening

The products of the main biochemical events of cheese ripening, e.g., peptides, free amino acids, organic acids, free short- and medium-chain fatty acids and their esters, and new substances resulting from their catabolism, e.g., alcohols, ketones, aldehydes, lactones, and amines, are mostly water-soluble; thus they are included in cheese WSE [11,26,27]. In the present study, cheese ripening assessment was based on spectral differences of samples in the regions that all the above substances absorb. Therefore, we focused on $1854\text{--}1381$ and $1192\text{--}760\text{ cm}^{-1}$ spectral regions, which include the “fingerprint” region and the carbonyl group and amide absorption, among others. Figure 1 shows typical FT-MIR spectra of the five different classes of lyophilized cheese WSE in the $2000\text{--}700\text{ cm}^{-1}$ spectral region. Table 1 shows that all the peaks appeared in $1854\text{--}1381$ and $1192\text{--}760\text{ cm}^{-1}$ regions and their assignments.

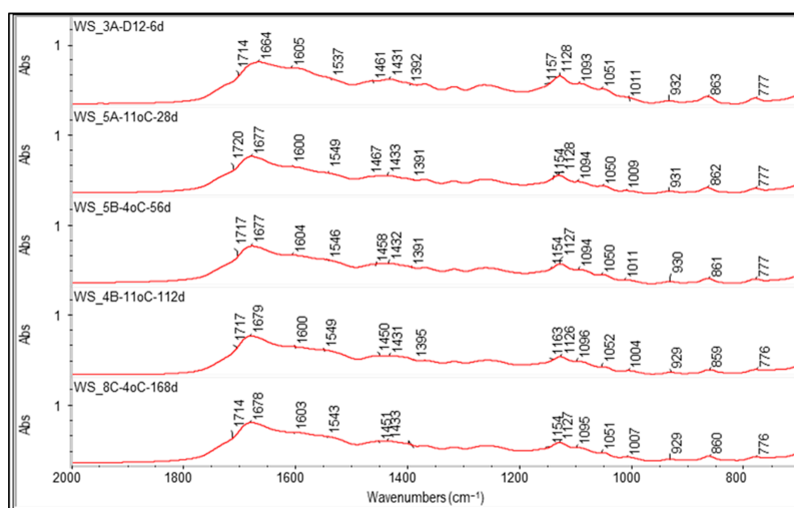


Figure 1. Fourier-transform infrared spectra in $2000\text{--}700\text{ cm}^{-1}$ spectral region of A, B and C cheese water-soluble extracts of five different classes, according to days of ripening; 6d, 6 days; 28d, 28 days; 56d, 56 days; 112d, 112 days; 168d, 168 days; A, full-fat sheep milk cheese; B, reduced-fat sheep milk cheese; C, reduced-fat sheep milk cheese fortified with sweet sheep buttermilk.

Table 1. Wavenumbers of the 15 peaks distinguished in 1854–1381 and 1192–760 cm^{−1} spectral regions of cheese water-soluble extracts and functional groups of the substances that absorb, among others, infrared light in the corresponding peak spectral regions.

Wavenumber (cm ^{−1})	Functional Group	Assignment	References
1720–1714	>C=O (stretching)	carboxylic acids	[10]
1679–1664	Amide I: >C=O (stretching) CN ₃ H ₅ ⁺ (asymmetric stretching)	esters of fatty acids peptides, proteins	[27] [8,11]
1605–1600	NH ₃ ⁺ (asymmetric deformation) COO [−] (asymmetric stretching)	arginine (side chain) free amino acids	[43] [44]
1549–1537	Amide II: N-H (bending) and C-N (stretching) COO [−] (asymmetric stretching) NH ₃ ⁺ (symmetric deformation) phenyl nucleus CH ₂ (scissoring) CH (bending)	peptides, proteins acidic amino acids (side chains) free amino acids aromatic amino acids isoleucine (side chain) lipids	[35,45] [33] [44] [45] [46] [30]
1467–1450	CH ₂ (in-plane bending) C-N (stretching) CH ₃ (asymmetric deformation)	proline, glutamic acid (side chains) proline (side chain) amines	[43] [43] [13]
1433–1431	COO [−] (symmetric stretching) CH (bending) CH ₃ (asymmetric deformation)	acidic amino acids lipids amines	[11,27] [30] [13]
1397–1391	COO [−] (symmetric stretching) CH (bending) CH ₃ (wagging)	free amino acids and salts amino acids (side chains) isoleucine (side chain)	[44] [13] [46]
1163–1154	C-O (stretching)	monosaccharides, ester link of lipids	[36]
1128–1126	C-OH (stretching) C-O (stretching)	lactose lipids	[36] [30]
	C-C (stretching)	organic acids	[8,10]
	S-O (asymmetric-symmetric stretching)	organic acids	[8,10]
1096–1093	N-CH (in-plane bending) NH ₂ (rocking/twisting) C-O (stretching)	proline (side chain) amines organic acids lactose	[47] [13] [8,10] [35]
	C-C (stretching) OH (bending) ring stretching	organic acids lactose	[8,10] [35]
1052–1050	C-O (stretching) C-C (stretching)	proline (side chain) organic acids organic acids	[48] [8,10] [8,10]
	CH (in-plane bending) of phenyl ring	phenylalanine	[49]
1011–1004	C-O (stretching) C-C (stretching)	organic acids organic acids	[8,10] [8,10]
	skeletal breath mode	phenylalanine	[49]
	C-N (stretching)	amines	[13]
932–929	C-O (stretching) C-C (stretching)	organic acids organic acids	[8,10] [8,10]
	OH (out-of-plane bending)	carboxylic acids	[10,12]

Table 1. Cont.

Wavenumber (cm^{-1})	Functional Group	Assignment	References
863–859	C-C (stretching)	proline (side chain)	[43]
	C-N (stretching)	proline (side chain)	[43]
	CH (out-of-plane bending) of phenyl ring	phenylalanine	[37]
777–776	ring vibration	pyranose compounds (saccharides)	[44]

3.1.2. Spectral Regions Related to Phospholipids

Sakkas et al., 2021 [42] proved that buttermilk addition in the cheese milk significantly increased ($p < 0.05$) the phospholipid content of cheese. Phospholipid basic structure includes a glycerol, linked to two fatty acids and one phosphate group [39]. We focused on three spectral regions to discriminate samples with different phospholipid content, that is the $3012\text{--}2851\text{ cm}^{-1}$ where the acyl chain of lipids absorbs, the $1854\text{--}1611\text{ cm}^{-1}$, where the carbonyl group of lipids absorbs, and the $1192\text{--}909\text{ cm}^{-1}$, where the phosphate group absorbs. Typical FT-MIR full spectra of cheese B and C WSE are presented in Figure 2. Table 2 shows all the peaks which appeared in the three aforementioned spectral regions and could be attributed to the functional groups of phospholipids, among other substances. The peaks at $2978\text{--}2971$ and $2883\text{--}2870\text{ cm}^{-1}$ have been assigned to the CH_3 asymmetric [50] and symmetric stretching [8,44], respectively, while the peak at $2936\text{--}2920\text{ cm}^{-1}$ has been attributed to the CH_2 asymmetric stretching [8,44]. The peak at $1720\text{--}1714\text{ cm}^{-1}$ has been associated with the stretching of the carbonyl group [51]. The absorption at $1160\text{--}1150\text{ cm}^{-1}$ can be assigned to the PO_2^- symmetric stretching [51] and the P=O stretching [44], while at $1096\text{--}1093\text{ cm}^{-1}$, can be attributed to the P-O-C asymmetric stretching [51] and the PO_2^- symmetric stretching [13,44]. The peaks at $1129\text{--}1126$, $1053\text{--}1050$ and $1014\text{--}998\text{ cm}^{-1}$ have been associated with the P-O-C asymmetric stretching [44,51], while the peak at $932\text{--}929\text{ cm}^{-1}$ can be assigned to the P-O stretching [44].

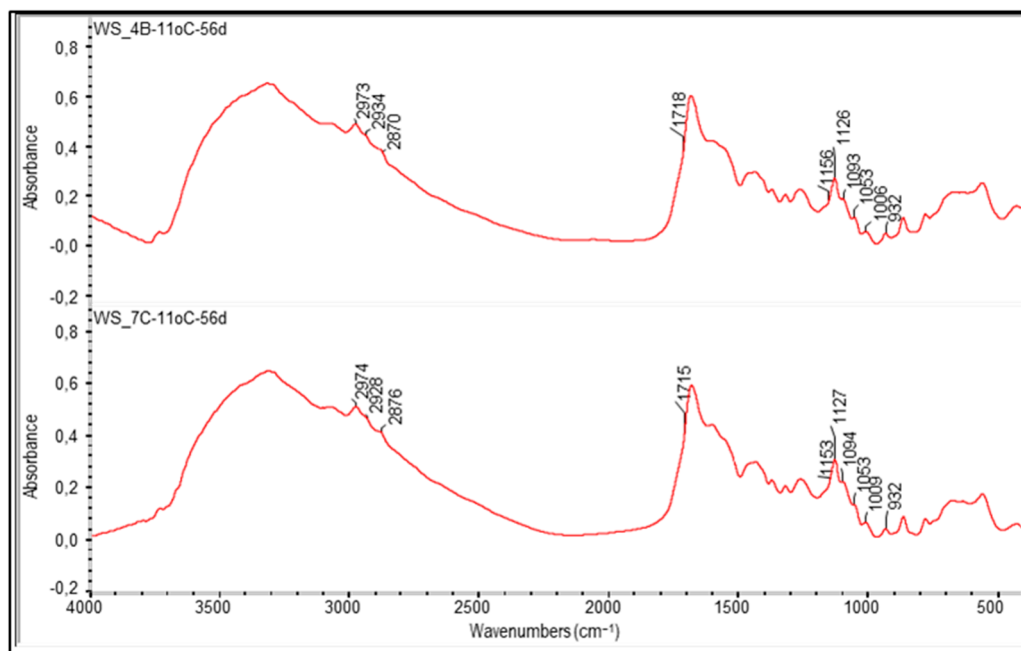


Figure 2. Fourier-transform infrared spectra in $4000\text{--}400\text{ cm}^{-1}$ spectral region of B (4B-11 °C-56d) and C (7C-11 °C-56d) cheese water-soluble extracts; B, reduced-fat sheep milk cheese; C, reduced-fat sheep milk cheese fortified with sweet sheep buttermilk.

Table 2. Wavenumbers of the 10 peaks distinguished in 3012–2851, 1854–1611 and 1192–909 cm^{-1} spectral regions of cheese water-soluble extracts could be attributed to the functional groups of phospholipids, among others.

Wavenumber (cm^{-1})	Functional Group	References
2978–2971	CH_3 (asymmetric stretching)	[50]
2936–2920	CH_2 (asymmetric stretching)	[8,44]
2883–2870	CH_3 (symmetric stretching)	[8,44]
1720–1714	C=O (stretching)	[51]
1160–1150	PO_2^- (symmetric stretching) P=O (stretching)	[51] [44]
1129–1126	P-O-C (asymmetric stretching)	[51]
1096–1093	P-O-C (asymmetric stretching)	[51]
1053–1050	PO_2^- (symmetric stretching)	[13,44]
1014–998	P-O-C (asymmetric stretching)	[44,51]
932–929	P-O-C (asymmetric stretching) P-O (stretching)	[44,51] [44]

3.2. Discriminant Analysis

Discriminant analysis of the samples was carried out by means of TQ Analyst software, which is a commercial and thus easy-to-use software and enables the direct external validation of a method using a spectrum test-set. The differences between spectra of different classes were limited and not distinct. Therefore, the discrimination of different classes could not be based on individual peaks and multivariate analysis was performed. After the separation of samples in the actual classes, the software applied the Mahalanobis algorithm to calculate the distances and create new calculated classes. Then each sample was inserted in a calculated class.

3.2.1. Discrimination Model of Ripening/Storage Stage

Forty-two calibration and 11 validation standards were classified correctly (97.7% and 73.3% respectively); the PI was 84.5% and all the external validation standards were classified correctly (100%). The distances of samples in the calculated classes varied from 0.615 to 1.180 in 6 d class, 0.732 to 1.200 in 28 d class, 0.686 to 1.244 in 56 d class, 0.675 to 1.182 in 112 d class, and 0.680 to 1.372 in 168 d class (Figure 3).

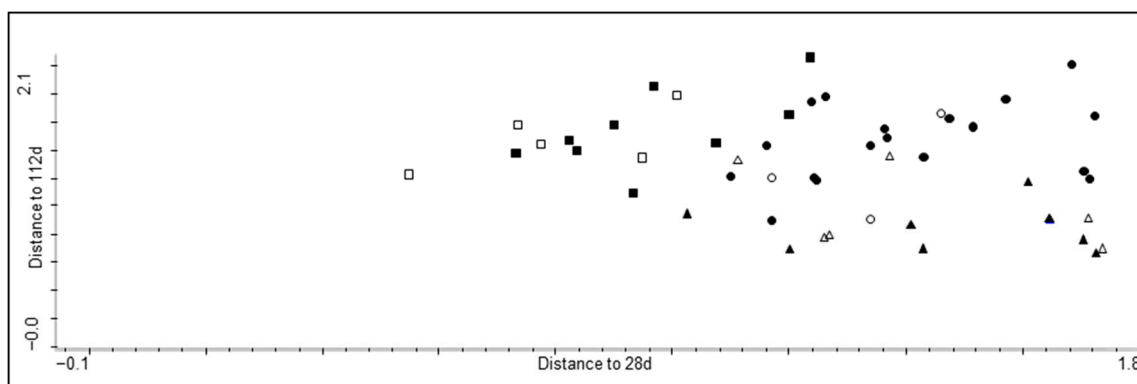


Figure 3. Scatter plot of the distances between lyophilized cheese water-soluble extracts of two different classes, according to days of ripening; 28 d, 28 days; 112 d, 112 days; ■, 28 d calibration; □, 28 d validation; ▲, 112 d calibration; △, 112 d validation; ●, other calibration; ○, other validation.

PC Scores measure the accuracy of the representation of each standard in the method by each PC used for method calibration. The calculated score values represent the multidimensional distance of each standard estimated on a PC. Figure 4 shows the PC Scores for the three-dimensional plot of the five classes of samples.

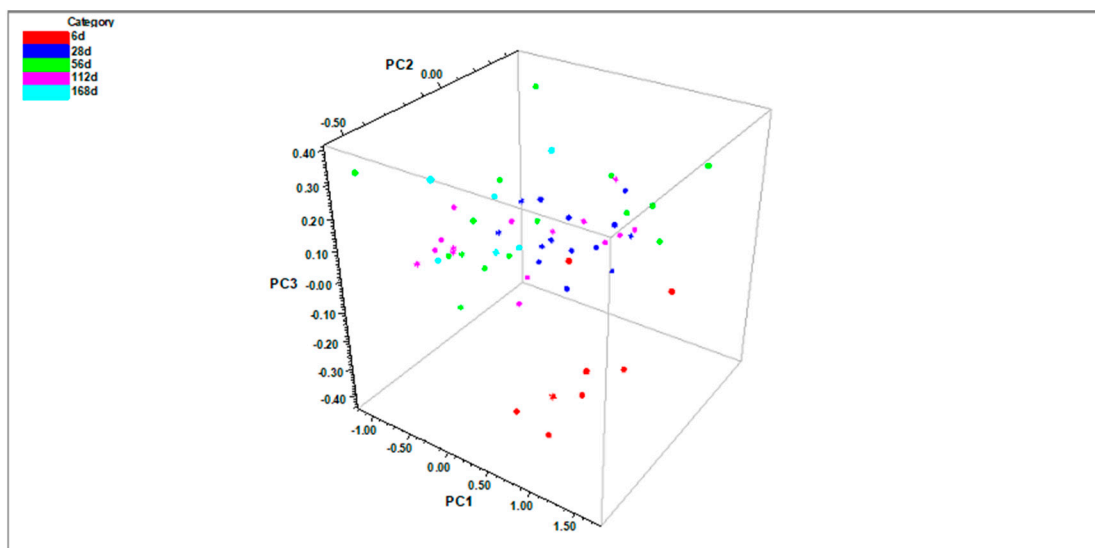


Figure 4. Principal Component Scores of three-dimensional plot of cheese water-soluble extracts of five different classes, according to days of ripening; PC, principal component; 6 d, 6 days; 28 d, 28 days; 56 d, 56 days; 112 d, 112 days; 168 d, 168 days.

3.2.2. Discrimination Model of Phospholipid Content

Twenty-four calibration and eight validation standards were classified correctly (92.3 and 80% respectively), the PI was 82.7% and five external validation standards were classified correctly (83.3%). The distances of cheeses B varied from 0.599 to 1.003 in calculated B class and the respective variation was 0.679 to 1.065 for cheeses C (Figure 5).

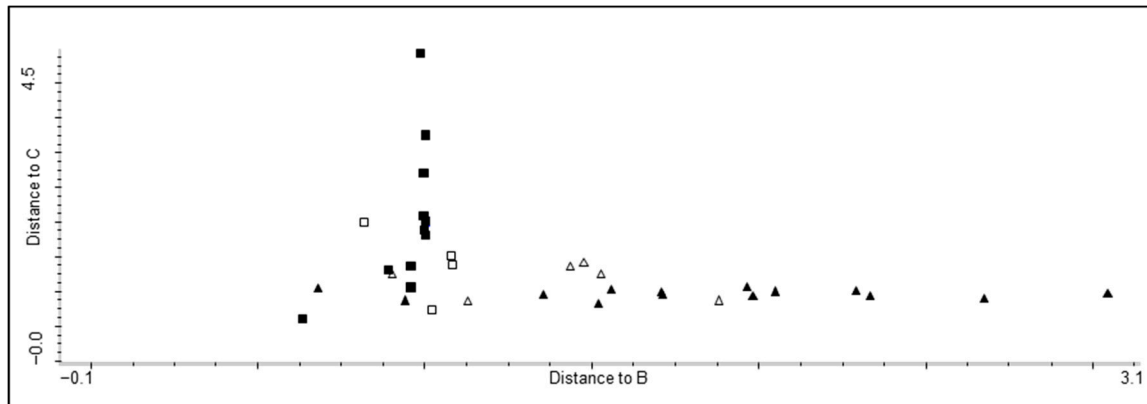


Figure 5. Scatter plot of the distances between water-soluble extracts of cheese B and C; B, reduced-fat sheep milk cheese; C, reduced-fat sheep milk cheese fortified with sweet sheep buttermilk; ■, B cheese calibration; □, B cheese validation; ▲, C cheese calibration; △, C cheese validation.

4. Discussion

4.1. Discrimination Model of Ripening/Storage Stage

Most compositional parameters and all proteolysis indices of the cheeses of the present study assessed by standard methods were significantly ($p < 0.05$) affected by cheese age [42]. These findings agree with the present FT-MIR analyses results and the successful discrimination of cheese WSE according to days of ripening. The discrimination of WSE was based on the absorbance regions of peptides and amino acids, among others. The nitrogenous components of cheese WSE mainly consist of residual whey proteins—which are not hydrolyzed during ripening—and of varying amounts of casein fragments—that is, large, medium, and small-size peptides and amino acids. Therefore, peptide bonds were expected to change with age in WSE, resulting in changes in the spectral regions where Amides I

and II absorb. Similarly, the protein and peptide catabolism that takes place during cheese ageing would have increased the absorbance of COO^- and NH_3^+ bands, resulting in changes in their spectral regions. All the aforementioned absorbance regions were included in the spectral regions used for the discriminant analysis of WSE samples, in addition to the absorbance regions of the other water-soluble products of ripening biochemical events. Consequently, the water-soluble extraction of cheeses is suitable for FT-MIR analysis and the developed statistical model is a reliable method for the discrimination of cheeses at different stages of ripening.

FT-MIR analysis of cheese water-soluble fractions has been reported by a few research groups. Subramanian et al., [6,11] discriminated cheddar cheese according to flavour quality and Kocaglu-Vurma et al., [12] differentiated Swiss cheeses by different manufacturers and production regions and developed predictive models for sensory evaluation. Koca et al., [10] analyzed Swiss cheese acidified water extract to determine short-chain free fatty acids and compared the results with that of direct cheese analysis. The measurement of cheese extract resulted in higher correlation with gas chromatography data and better calibration models compared to direct cheese measurement, in which the non-removal of high fat and protein contents caused interferences. Moreover, the authors suggested that an extraction procedure resolves the problem of cheese heterogeneity in sampling. Martín-del-Campo et al., [35] analyzed the defatted suspensions and their acid soluble nitrogen extracts of Camembert-type cheeses ripened up to 27 days. They discriminated samples of different age and determined the days of ripening with one day error; however, they reported no improvement of the analysis results using cheese fractions. Subramanian et al. [27] and Chen et al., [37] performed FT-MIR analysis of water/chloroform/ethanol extracts of cheddar and Swiss cheeses, respectively, and developed models for cheese classification according to their age, based on differences in the $1800\text{--}900\text{ cm}^{-1}$ spectral region. The former research group also developed prediction models of cheese age and of the levels of amino acids and organic acids. They reported good correlation with cheese age and gas chromatography and HPLC data and concluded that cheese extraction improved the signal from water-soluble compounds.

4.2. Discrimination Model of Phospholipid Content

The present study aimed to establish the spectral regions of phospholipid absorbance in cheese extract and to develop a discriminating method based on samples with different phospholipid content. As mentioned before, phospholipids are amphipolar molecules, which emerges the question whether they totally or merely migrated to water phase during cheese water extraction. Moreover, cheese extract also contains phosphopeptides [52] which absorb light at the phosphate group region ($1192\text{--}909\text{ cm}^{-1}$) and free short- and medium-chain fatty acids which absorb light at the acyl chain ($3012\text{--}2851\text{ cm}^{-1}$) and carbonyl group ($1854\text{--}1611\text{ cm}^{-1}$) regions. The absorption of those substances at the same regions with phospholipids means that they may contribute to the signal produced by phospholipid absorption, causing difficulties in the development of the discrimination model. In order to address the aforementioned difficulties, samples of markedly different phospholipid content, namely cheeses B and C, were used for the development of the discrimination model. Sakkas et al. [42] have evaluated the phospholipid content in cheeses B and C by a direct method and they reported that it was significantly higher in fat, cheese and dry matter of cheese C compared to that of cheese B. In particular, the phospholipid contents of cheeses B and C at 28d were 378 ± 4 and $569 \pm 11\text{ mg}/100\text{ g}$ fat, 43 ± 1 and $67 \pm 1\text{ mg}/100\text{ g}$ cheese and 94 ± 1 and $150 \pm 3\text{ mg}/100\text{ g}$ dry matter, respectively. Regarding the age of 112 d, the respective phospholipid contents of cheeses B and C were 401 ± 5 and $579 \pm 6\text{ mg}/100\text{ g}$ fat, 52 ± 1 and $69 \pm 1\text{ mg}/100\text{ g}$ cheese and 107 ± 2 and $151 \pm 1\text{ mg}/100\text{ g}$ dry matter. This difference was due to the addition of sweet buttermilk in cheese milk C since buttermilk is considered a rich source of phospholipids due to its high content in milk fat globule membrane material [39,42,53].

Our results showed that the discrimination model based on spectral regions related to phospholipids is robust and can differentiate WSE from cheeses with different phospholipid content. It resulted in a 92.3% correct classification of calibration standards, 80% correct classification of validation standards, 82.7% PI and 83.3% correct classification of external validation standards. Therefore, the discrimination was due to differences in phospholipid absorption among samples, indicating that a significant portion of phospholipids shifts to the aqueous part during cheese water extraction. Moreover, the suitability of cheese WSE for FT-MIR assessment of cheese phospholipid content is demonstrated similarly to the discrimination model developed for the ripening stage. Further research is needed to investigate the application of FT-MIR to phospholipid analysis, aiming to replace the current time—and cost-consuming analytical techniques and to assess the effectiveness of the present method in the differentiation of cheeses with more variable phospholipid contents.

5. Conclusions

Two FT-MIR robust models, double validated, were developed in this study for the discrimination of semi-hard sheep milk cheeses according to their ripening time or phospholipid content, by analyzing a simple lyophilized cheese water-extract (WSE). Double validation (internal; external) increases the robustness of the model and therefore its validity. The results of both models showed that cheese WSE is suitable for FT-MIR cheese analysis because: (i1) it is simple, (i2) it overcomes the interferences of fat and protein and the sampling difficulties resulting from cheese heterogeneity, (i3) it does not use organic solvents, and (i4) analysis is focused on water-soluble substances. The novelty of the present work is the use of FT-MIR spectra of the water-soluble extract for the assessment (1) of the ripening of a sheep milk cheese, and (2) of the phospholipid content of cheese. The rapid, plain and low-cost model developed in this work for the differentiation of cheeses by their ripening time could be very useful for scientific research and the cheese industry. It could help to replace the time consuming and expensive analytical methods used currently for the monitoring of ripening, which is an important element of the quality control of cheese. By the second developed model, cheeses with different phospholipid content were discriminated and it was shown that a considerable part of phospholipids migrates to the aqueous phase during cheese extraction. Further research for the development of a quantitative or measurement method based on FT-MIR analysis of cheese WSE would be of great interest considering the importance of dairy phospholipids from a technological and dietary point of view. The same holds true for the investigation of the implementation of FT-MIR in phospholipid analysis, which could replace the current time intensive and costly analytical techniques. The major strength of the present study is the robustness of the developed models. In this respect, their application in the analysis of various cheese samples is a future research perspective.

Author Contributions: Conceptualization, C.S.P. and G.M.; methodology, L.S., G.M. and C.S.P.; validation, L.S. and C.S.P.; formal analysis, L.S. and C.S.P.; investigation, L.S. and G.M.; resources, G.M. and C.S.P.; data curation, L.S. and C.S.P.; writing—original draft preparation, L.S.; writing—review and editing, L.S., G.M. and C.S.P.; visualization, L.S., G.M. and C.S.P.; supervision, C.S.P.; project administration, G.M. and C.S.P.; funding acquisition, G.M. and C.S.P. All authors have read and agreed to the published version of the manuscript.

Funding: This research received no external funding.

Data Availability Statement: The datasets generated for this study are available on request to the corresponding author.

Conflicts of Interest: The authors declare no conflict of interest.

References

1. Kamal, M.; Karoui, R. Analytical methods coupled with chemometric tools for determining the authenticity and detecting the adulteration of dairy products: A review. *Trends Food Sci. Technol.* **2015**, *46*, 27–48. [[CrossRef](#)]
2. Karoui, R.; Mazerolles, G.; Dufour, É. Spectroscopic techniques coupled with chemometric tools for structure and texture determinations in dairy products. *Int. Dairy J.* **2003**, *13*, 607–620. [[CrossRef](#)]
3. De Marchi, M.; Penasa, M.; Zidi, A.; Manuelian, C.L. Invited review: Use of infrared technologies for the assessment of dairy products—Applications and perspectives. *J. Dairy Sci.* **2018**, *101*, 10589–10604. [[CrossRef](#)] [[PubMed](#)]
4. Karoui, R.; De Baerdemaeker, J. A review of the analytical methods coupled with chemometric tools for the determination of the quality and identity of dairy products. *Food Chem.* **2007**, *102*, 621–640. [[CrossRef](#)]
5. Pappas, C.S.; Tarantilis, P.A.; Moschopoulou, E.; Moatsou, G.; Kandarakis, I.; Polissiou, M.G. Identification and differentiation of goat and sheep milk based on diffuse reflectance infrared Fourier transform spectroscopy (DRIFTS) using cluster analysis. *Food Chem.* **2008**, *106*, 1271–1277. [[CrossRef](#)]
6. Subramanian, A.; Harper, W.J.; Rodriguez-Saona, L.E. Rapid Prediction of Composition and Flavor Quality of Cheddar Cheese Using ATR-FTIR Spectroscopy. *J. Food Sci.* **2009**, *74*, 292–297. [[CrossRef](#)] [[PubMed](#)]
7. Rodriguez-Saona, L.E.; Koca, N.; Harper, W.J.; Alvarez, V.B. Rapid Determination of Swiss Cheese Composition by Fourier Transform Infrared/Attenuated Total Reflectance Spectroscopy. *J. Dairy Sci.* **2006**, *89*, 1407–1412. [[CrossRef](#)]
8. Karoui, R.; Mouazen, A.M.; Dufour, É.; Pillonel, L.; Picque, D.; Bosset, J.-O.; De Baerdemaeker, J. Mid-infrared spectrometry: A tool for the determination of chemical parameters in Emmental cheeses produced during winter. *Lait* **2006**, *86*, 83–97. [[CrossRef](#)]
9. Karoui, R.; Mouazen, A.M.; Dufour, É.; Schoonheydt, R.; De Baerdemaeker, J. A comparison and joint use of VIS-NIR and MIR spectroscopic methods for the determination of some chemical parameters in soft cheeses at external and central zones: A preliminary study. *Eur. Food Res. Technol.* **2006**, *223*, 363–371. [[CrossRef](#)]
10. Koca, N.; Rodriguez-Saona, L.E.; Harper, W.J.; Alvarez, V.B. Application of Fourier Transform Infrared Spectroscopy for Monitoring Short-Chain Free Fatty Acids in Swiss Cheese. *J. Dairy Sci.* **2007**, *90*, 3596–3603. [[CrossRef](#)]
11. Subramanian, A.; Harper, W.J.; Rodriguez-Saona, L.E. Cheddar cheese classification based on flavor quality using a novel extraction method and Fourier transform infrared spectroscopy. *J. Dairy Sci.* **2009**, *92*, 87–94. [[CrossRef](#)]
12. Kocauoglu-Vurma, N.A.; Eliardi, A.; Drake, M.A.; Rodriguez-Saona, L.E.; Harper, W.J. Rapid Profiling of Swiss Cheese by Attenuated Total Reflectance (ATR) Infrared Spectroscopy and Descriptive Sensory Analysis. *J. Food Sci.* **2009**, *74*, S232–S239. [[CrossRef](#)] [[PubMed](#)]
13. Papadopoulou, O.S.; Argyri, A.A.; Varzakas, E.E.; Tassou, C.C.; Chorianopoulos, N.G. Greek functional Feta cheese: Enhancing quality and safety using a *Lactobacillus plantarum* strain with probiotic potential. *Food Microbiol.* **2018**, *74*, 21–33. [[CrossRef](#)]
14. Lerma-García, M.J.; Gori, A.; Cerretani, L.; Simó-Alfonso, E.F.; Caboni, M.F. Classification of Pecorino cheeses produced in Italy according to their ripening time and manufacturing technique using Fourier transform infrared spectroscopy. *J. Dairy Sci.* **2010**, *93*, 4490–4496. [[CrossRef](#)] [[PubMed](#)]
15. Andersen, C.M.; Frøst, M.B.; Viereck, N. Spectroscopic characterization of low- and non-fat cream cheeses. *Int. Dairy J.* **2010**, *20*, 32–39. [[CrossRef](#)]
16. Guerzoni, M.E.; Vannini, L.; Lopez, C.C.; Lanciotti, R.; Suzzi, G.; Gianotti, A. Effect of High Pressure Homogenization on Microbial and Chemico-Physical Characteristics of Goat Cheeses. *J. Dairy Sci.* **1999**, *82*, 851–862. [[CrossRef](#)]
17. Karoui, R.; Dufour, É.; Pillonel, L.; Picque, D.; Cattenoz, D.; Bosset, J.-O. Determining the geographic origin of Emmental cheeses produced during winter and summer using a technique based on the concatenation of MIR and fluorescence spectroscopic data. *Eur. Food Res. Technol.* **2004**, *219*, 184–189. [[CrossRef](#)]
18. Karoui, R.; Dufour, É.; Pillonel, L.; Picque, D.; Cattenoz, T.; Bosset, J.-O. Fluorescence and infrared spectroscopies: A tool for the determination of the geographic origin of Emmental cheeses manufactured during summer. *Lait* **2004**, *84*, 359–374. [[CrossRef](#)]
19. Karoui, R.; Mazerolles, G.; Bosset, J.-O.; De Baerdemaeker, J.; Dufour, E. Utilisation of mid-infrared spectroscopy for determination of the geographic origin of Gruyère PDO and L’Etivaz PDO Swiss cheeses. *Food Chem.* **2007**, *105*, 847–854. [[CrossRef](#)]
20. Cevoli, C.; Gori, A.; Nocetti, M.; Cuibus, L.; Caboni, M.F.; Fabbri, A. FT-NIR and FT-MIR spectroscopy to discriminate competitors, non compliance and compliance grated Parmigiano Reggiano cheese. *Food Res. Int.* **2013**, *52*, 214–220. [[CrossRef](#)]
21. Gori, A.; Maggio, R.M.; Cerretani, L.; Nocetti, M.; Caboni, M.F. Discrimination of grated cheeses by Fourier transform infrared spectroscopy coupled with chemometric techniques. *Int. Dairy J.* **2012**, *23*, 115–120. [[CrossRef](#)]
22. Boubellouta, T.; Karoui, R.; Lebecque, A.; Dufour, E. Utilisation of attenuated total reflectance MIR and front-face fluorescence spectroscopies for the identification of Saint-Nectaire cheeses varying by manufacturing conditions. *Eur. Food Res. Technol.* **2010**, *231*, 873–882. [[CrossRef](#)]
23. Cuibus, L.; Maggio, R.; Mureşan, V.; Diaconeasa, Z.; Fetea, F.; Socaciu, C. Preliminary Discrimination of Cheese Adulteration by FT-IR Spectroscopy. *Bull. Univ. Agric. Sci. Veter. Med. Cluj-Napoca. Food Sci. Technol.* **2014**, *71*, 142–146. [[CrossRef](#)]
24. Leite, A.I.N.; Pereira, C.G.; Andrade, J.; Vicentini, N.M.; Bell, M.J.V.; Anjos, V. FTIR-ATR spectroscopy as a tool for the rapid detection of adulterations in butter cheeses. *LWT* **2019**, *109*, 63–69. [[CrossRef](#)]
25. Sousa, M.J.; Ardö, Y.; McSweeney, P.L.H. Advances in the study of proteolysis during cheese ripening. *Int. Dairy J.* **2001**, *11*, 327–345. [[CrossRef](#)]
26. McSweeney, P.L.H.; Sousa, M.J. Biochemical pathways for the production of flavour compounds in cheeses during ripening: A review. *Lait* **2000**, *80*, 293–324. [[CrossRef](#)]

27. Subramanian, A.; Alvarez, V.B.; Harper, W.J.; Rodriguez-Saona, L.E. Monitoring amino acids, organic acids, and ripening changes in Cheddar cheese using Fourier-transform infrared spectroscopy. *Int. Dairy J.* **2011**, *21*, 434–440. [[CrossRef](#)]
28. Martín-Del-Campo, S.T.; Picque, D.; Cosío-Ramírez, R.; Corrieu, G. Evaluation of Chemical Parameters in Soft Mold-Ripened Cheese During Ripening by Mid-Infrared Spectroscopy. *J. Dairy Sci.* **2007**, *90*, 3018–3027. [[CrossRef](#)]
29. Baghdadi, F.; Aminifar, M.; Farhoodi, M.; Abadi, S.S.A. Study of macromolecular interactions in low-fat brined cheese modified with Zedu gum. *Int. J. Dairy Technol.* **2018**, *71*, 382–394. [[CrossRef](#)]
30. Chen, M.; Irudayaraj, J.; McMahon, D.J. Examination of Full Fat and Reduced Fat Cheddar Cheese During Ripening by Fourier Transform Infrared Spectroscopy. *J. Dairy Sci.* **1998**, *81*, 2791–2797. [[CrossRef](#)]
31. Lanciotti, R.; Vannini, L.; López, C.C.; Gobbetti, M.; Guerzoni, M.E. Evaluation of the ability of *Yarrowia lipolytica* to impart strain-dependent characteristics to cheese when used as a ripening adjunct. *Int. J. Dairy Technol.* **2005**, *58*, 89–99. [[CrossRef](#)]
32. Dufour, É.; Mazerolles, G.; Devaux, M.F.; Duboz, G.; Dupoyer, M.H.; Riou, N. Phase transition of triglycerides during semi-hard cheese ripening. *Int. Dairy J.* **2000**, *10*, 81–93. [[CrossRef](#)]
33. Duboz, G.; Riou, N.M.; Mazerolles, G.; Devaux, M.-F.; Dupoyer, M.-H.; Dufour, E. Infrared and fluorescence spectroscopy for monitoring protein structure and interaction changes during cheese ripening. *Lait* **2001**, *81*, 509–527. [[CrossRef](#)]
34. Cattaneo, T.M.P.; Giardina, C.; Sinelli, N.; Riva, M.; Giangiacomo, R. Application of FT-NIR and FT-IR spectroscopy to study the shelf-life of Crescenza cheese. *Int. Dairy J.* **2005**, *15*, 693–700. [[CrossRef](#)]
35. Martín-Del-Campo, S.T.; Picque, D.; Cosío-Ramírez, R.; Corrieu, G. Middle infrared spectroscopy characterization of ripening stages of Camembert-type cheeses. *Int. Dairy J.* **2007**, *17*, 835–845. [[CrossRef](#)]
36. Del Campo, S.T.; Bonnaire, N.; Picque, D.; Corrieu, G. Initial studies into the characterisation of ripening stages of Emmental cheeses by mid-infrared spectroscopy. *Dairy Sci. Technol.* **2009**, *89*, 155–167. [[CrossRef](#)]
37. Chen, G.; Kocaoglu-Vurma, N.A.; Harper, W.J.; Rodriguez-Saona, L.E. Application of infrared microspectroscopy and multivariate analysis for monitoring the effect of adjunct cultures during Swiss cheese ripening. *J. Dairy Sci.* **2009**, *92*, 3575–3584. [[CrossRef](#)]
38. Andrade, J.; Pereira, C.G.; Ranquine, T.; Azarias, C.A.; Bell, M.J.V.; Anjos, V.D.C.D. Long-Term Ripening Evaluation of Ewes' Cheeses by Fourier-Transformed Infrared Spectroscopy under Real Industrial Conditions. *J. Spectrosc.* **2018**, *2018*, 1381864. [[CrossRef](#)]
39. Rombaut, R.; Dewettinck, K. Properties, analysis and purification of milk polar lipids. *Int. Dairy J.* **2006**, *16*, 1362–1373. [[CrossRef](#)]
40. Nilsson, Å.; Duan, R.-D.; Ohlsson, L. Digestion and Absorption of Milk Phospholipids in Newborns and Adults. *Front. Nutr.* **2021**, *8*, 724006. [[CrossRef](#)] [[PubMed](#)]
41. Hauff, S.; Vetter, W. Quantification of fatty acids as methyl esters and phospholipids in cheese samples after separation of triacylglycerides and phospholipids. *Anal. Chim. Acta* **2009**, *636*, 229–235. [[CrossRef](#)] [[PubMed](#)]
42. Sakkas, L.; Alatini, E.; Moatsou, G. Use of sweet sheep buttermilk in the manufacture of reduced-fat sheep milk cheese. *Int. Dairy J.* **2021**, *120*, 105079. [[CrossRef](#)]
43. Barth, A. The infrared absorption of amino acid side chains. *Prog. Biophys. Mol. Biol.* **2000**, *74*, 141–173. [[CrossRef](#)]
44. Socrates, G. *Infrared and Raman Characteristic Group Frequencies: Tables and Charts*, 3rd ed.; John Wiley and Sons: West Sussex, UK, 2001; pp. 229–338.
45. Pappas, C.; Sakkas, L.; Moschopoulou, E.; Moatsou, G. Direct determination of lactulose in heat-treated milk using diffuse reflectance infrared Fourier transform spectroscopy and partial least squares regression. *Int. J. Dairy Technol.* **2015**, *68*, 448–453. [[CrossRef](#)]
46. Moorthi, P.P.; Gunasekaran, S.; Ramkumar, G.R. Vibrational spectroscopic studies of Isoleucine by quantum chemical calculations. *Spectrochim. Acta Part A Mol. Biomol. Spectrosc.* **2014**, *124*, 365–374. [[CrossRef](#)] [[PubMed](#)]
47. Borah, B.; Devi, T.G. Vibrational study on the molecular interaction of L-Proline and Para-Aminobenzoic acid. *J. Mol. Struct.* **2020**, *1203*, 127396. [[CrossRef](#)]
48. Mary, S.Y.; Ushakumari, L.; Harikumar, B.; Varghese, H.T.; Panicker, C.Y. FT-IR, FT-raman and SERS spectra of L-proline. *J. Iran. Chem. Soc.* **2009**, *6*, 138–144. [[CrossRef](#)]
49. Olsztyńska-Janus, S.; Komorowska, M. Conformational changes of l-phenylalanine induced by near infrared radiation. ATR-FTIR studies. *Struct. Chem.* **2012**, *23*, 1399–1407. [[CrossRef](#)]
50. Coates, J. Interpretation of infrared spectra: A practical approach. In *Encyclopedia of Analytical Chemistry*; Meyers, R.A., Ed.; John Wiley and Sons Ltd.: Chichester, UK, 2000; Volume 12, pp. 10815–10837.
51. Nzai, J.M.; Proctor, A. Determination of phospholipids in vegetable oil by fourier transform infrared spectroscopy. *J. Am. Oil Chem. Soc.* **1998**, *75*, 1281–1289. [[CrossRef](#)]
52. Ardö, Y.; Lilbæk, H.; Kristiansen, K.R.; Zakora, M.; Otte, J. Identification of large phosphopeptides from β-casein that characteristically accumulate during ripening of the semi-hard cheese Herrgård. *Int. Dairy J.* **2007**, *17*, 513–524. [[CrossRef](#)]
53. Ali, A.H. Current knowledge of buttermilk: Composition, applications in the food industry, nutritional and beneficial health characteristics. *Int. J. Dairy Technol.* **2019**, *72*, 169–182. [[CrossRef](#)]